State selective electron transport through electronic surface states of 6*H*-SiC(0001)-3×3

G. Baffou, A. J. Mayne, G. Comtet, and G. Dujardin
Laboratoire de Photophysique Moléculaire, Bâtiment 210, Université Paris-Sud, 91405 Orsay, France
(Received 11 February 2008; published 14 April 2008)

We investigate charge transport through electronic surface states of the 6*H*-SiC(0001)-3×3 surface. Three intrinsic surface states are located within the wide bulk band gap, in which two (S_1 and U_1) arise from strongly correlated electronic states and the third (S_2) has negligible electron correlation effects. Combined conductance and luminescence experiments with the scanning tunneling microscope show that the Mott-Hubbard surface states (S_1 and U_1) have a high resistance (1.0 GΩ), while the noncorrelated state (S_2) has a negligible resistance. Consequently, current can be selectively transported through any of these three surface states.

DOI: 10.1103/PhysRevB.77.165320 PACS number(s): 73.20.At, 73.25.+i, 78.60.Fi, 68.37.Ef

I. INTRODUCTION

Charge transport through electronic surface states[1–4] is becoming of utmost importance as the thickness of materials decreases. A number of recent results, such as in thin silicon layers on insulators[5] and studies of the properties of thin epitaxial graphene layers on silicon carbide,[6–8] suggest that future electronic devices of smaller size and higher operating speeds will be possible. In this context, a clear atomic-scale understanding of charge transport at surfaces and interfaces is vital. Charge transport through electronic surface states is complex on many semiconductor surfaces, such as silicon,[1,9] germanium,[10,11] and diamond.[12–15] Indeed, these studies show the difficulty to unambiguously distinguish between surface state, subsurface, or bulk conduction. The wide band gap 6*H*-SiC(0001)-3×3 surface is the ideal system to investigate such charge transport through electronic surface states, in particular, the influence of electron correlation effects[16–19] on the surface conduction. Indeed, three intrinsic surface states are located within the bulk band gap, in which two (S_1 and U_1) arise from strongly correlated electronic states and the third (S_2) has negligible electron correlation effects.[20,21] The morphology of the surface states has a significant influence on the electronic transport properties. Two features have to be distinguished: (i) the high localization induces strong electronic correlations, which are responsible of a gap opening in the energy distribution and the formation of two distinct surface states U_1 and S_1, the so-called Mott-Hubbard electronic states, and (ii) the weak overlap between neighboring silicon adatoms is responsible for a reduced electronic mobility along the semiconductor surface through U_1 or S_1. Both these features have, therefore, an influence on the electronic conductivity. In this paper, a combination of conductance and luminescence experiments with the scanning tunneling microscope (STM) is used to demonstrate that the Mott-Hubbard surface states (S_1 and U_1) have a high resistance (1.0 GΩ), whereas the noncorrelated state (S_2) has a negligible resistance. These results exemplify the role of electron localization and correlation in surface conductance and show that selective electron transport through surface states is possible.

II. EXPERIMENT

The STM experiments were performed at room temperature in an ultrahigh vacuum chamber (base pressure of 3 $\times 10^{-11}$ Torr) by using electrochemically etched Ag tips. A highly nitrogen-doped (density of 3×10^{18} cm^{-3}) *n*-type 6*H*-SiC(0001) single crystal wafer was used. After outgassing, the SiC sample was flashed at 1100 °C to remove the native oxide, followed by silicon deposition on the surface at 650 °C for a few minutes.[22] Annealing at the same temperature (650 °C) for 10 min led to a well reconstructed 3×3 surface, as specified by a sharp low energy electron diffraction pattern. The light emitted from the sample under the STM tip was collected at 32° from the surface by a system composed of three lenses mounted in vacuum. The collected light was transmitted through an optical fiber, dispersed by a grating spectrometer, and detected by a liquid nitrogen cooled charge-coupled device camera. The overall transmission of the optical setup is around 12% in the photon energy range of 1.2–3.2 eV.

III. RESULTS AND DISCUSSION

A. *I*(*V*) spectroscopy of surface states

The STM topography of the silicon terminated 6*H*-SiC(0001)-3×3 surface is shown in the inset of Fig. 1(a). The 3×3 reconstruction exhibits silicon dangling bonds (DBs) (seen as bright protrusions in STM topographies) located on top of pyramidlike structures[23,24] separated by 9.24 Å. Figure 1(a) shows a series of equivalent $I(V)$ spectra obtained with a silver tip for a tunnel current set point of 300 pA. All spectra are taken on top of the silicon DBs [as the inset in Fig. 1(a) shows] to avoid the defects. Thus, the dispersion of the corresponding $I(V)$ curves is very small [Fig. 1(a)]. There is a very little difference between on top of a DB and between DBs; however, spectra taken on defect sites can be very different, displaying a completely different profile. The reliability of the spectra was noticeably tip dependent and a good STM resolution associated with a low current noise is essential to expect reliable measurements. Normalized $(dI/dV)/(I/V)$ spectra acquired at different tunnel current set points, i.e., different tip-sample distances, are presented in Fig. 1(b). Three surface states, U_1, S_1, and S_2, observed at 0.5, −0.5, and −1.5 eV, respectively (for the lowest tunnel current set point of 0.1 nA), have energies relative to the Fermi level in very good agreement with angle resolved inverse and direct photoemission

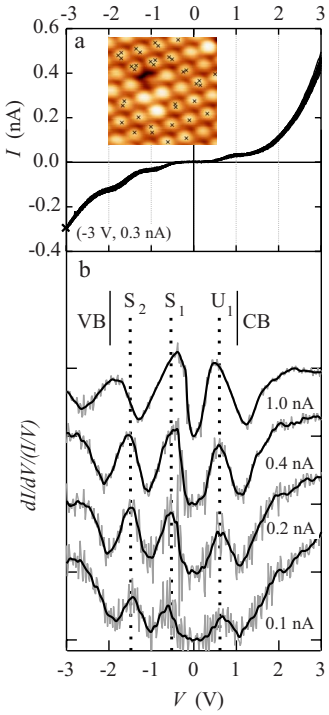

FIG. 1. (Color online) (a) A series of $I(V)$ spectroscopy curves taken on the 6H-SiC(0001)-3×3 surface. The crosses on the 5.5×5.5 nm^2 STM topography (inset, $V=-3.0$ V, $I=0.3$ nA) mark the individual curves. (b) $dI/dV/(I/V)$ STM spectroscopy curves recorded at different set points ($I=0.1$, 0.2, 0.4, and 1.0 nA, $V=-3$ V) showing the intrinsic U_1, S_1, and S_2 surface states lying in the bulk band gap. The VB maximum energy and conduction band minimum energy are indicated by vertical bars.

spectroscopy.[21] Decreasing the tip-sample distance causes a displacement toward higher binding energies of the S_2 surface state due to surface band bending.[17] U_1, S_1, and S_2 surface states have energies located within the bulk band gap (3.0 eV width).[21] It has been shown from a Mott-Hubbard model[18] that the occupied S_1 and unoccupied U_1 surface states arise from strong electron correlation effects of electronic states localized at the Si adatom sites. The very small observed dispersion of the corresponding bands[21] is the first indication that charge transport through the S_1 and U_1 surface states should be weak. On the contrary, the S_2 surface band exhibits a clear band dispersion,[21] indicating that charge transport should be more favorable through S_2. In our results, only three peaks are observed. The ARUPS (angular resolved ultraviolet photoemission spectroscopy) work suggested the existence of a fourth peak in the spectra, which could be attributed to an S_3 state at −1.9 eV.[21] This was not seen in our spectra due to the presence of the valence band (VB) edge at this energy.

B. $I(Z)$ spectroscopy

The conductance of the various surface states can be directly tested by $I(Z)$ STM spectroscopy. $I(Z)$ spectroscopy is performed at constant surface voltage by measuring the tunnel current I as a function of the tip displacement Z. Note

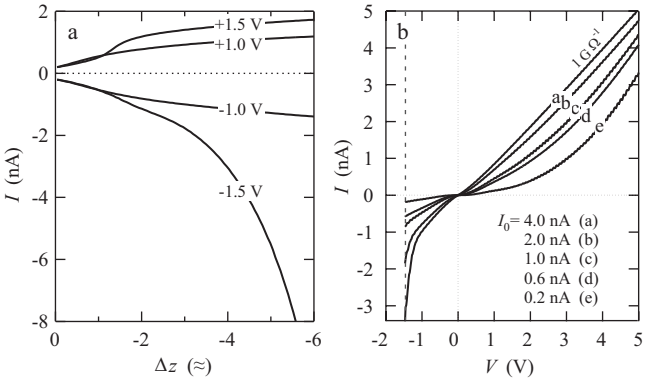

FIG. 2. (a) $I(Z)$ curves recorded at various sample voltages, $V=1.5$, 1.0, −1.0, and −1.5 V, and (b) $I(V)$ curves recorded at a single sample voltage, $V=-1.5$ V, for different tunnel current set points [(a)–(e)] from $I=4.0$ nA to $I=0.2$ nA. The resistance of 1 GΩ^{-1} is estimated from the slope of curve (a).

that the initial tip-sample distance (determined by V and I) is not known. $I(Z)$ spectra recorded at constant sample voltages V of +1.5, +1.0, −1.0, and −1.5 V are shown in Fig. 2(a). These voltages were chosen to probe the conductance of the U_1 state ($V=+1.5$ and +1.0 V), the S_1 state ($V=-1.0$ V), and the S_1+S_2 surface states ($V=-1.5$ V). At +1.5, +1.0, and −1.0 V voltages, the tunnel current becomes saturated as the tip approaches the surface. On the contrary, at −1.5 V, the $I(Z)$ curve shows an exponential-like decay as a function of the tip displacement[25] such that high tunnel currents up to 50 nA could be obtained for small Z values. However, the decay is less rapid than expected (less current passes when the tip-surface distance decreases). This can be explained by band bending due to the electric field between the tip and surface. An indication of this is that S_2 is seen to shift toward −2 eV as the set-point current is increased. The shapes of the $I(Z)$ curves at +1.5, +1.0, and −1.0 V cannot be accounted for by the tunnel barrier transmission alone. It is ascribed to a high resistance of the surface across which an important proportion of the applied voltage drops, resulting in a reduced voltage between the tip and the surface and subsequent limitation of the tunnel current. This is confirmed by the $I(V)$ curves recorded at small tip-surface distances.

C. Surface state resistance measurements by $I(V)$ spectroscopy at small tip-surface distances

In STM experiments, the surface voltage V is defined as the voltage drop between the sample holder and the STM tip.[26] V is the sum of the voltage drop across the sample, V_S, and the voltage drop, V_t, across the tunnel barrier,

$$V = V_S + V_t = (R_S + R_t)I = RI.$$

Usually, in STM experiments, the sample resistance R_S is negligible compared to the resistance of the tunnel barrier, R_t, such that $V \sim R_t I$. The corresponding $I(V)$ curves are markedly nonlinear (see Fig. 1) since R_t (Z,V) depends on the surface voltage V (Z is fixed by the voltage and current set point). On the contrary, when the sample resistance R_S is higher than the tunnel barrier resistance, R_t (Z,V), $V \sim R_S I$

and linear $I(V)$ curves might be observed, as we will demonstrate in what follows.

Figure 2(b) shows a series of $I(V)$ curves recorded at various tip-surface distances. The set-point voltage is $V=-1.5$ V and tunnel current set points were varied from 0.2 to 4 nA. This corresponds to much smaller tip-surface distances than for $I(V)$ curves in Fig. 1, where the set points are $V=-3$ V and $I=0.5$ nA. For the smallest tip-surface distances (set point $V=-3$ V, $I_0=4.0$ nA), the $I(V)$ curve shows a linear behavior in the range from +5 to −1 V and a strongly nonlinear behavior below −1 V. This means that in the range from +5 to −1 V, i.e., where U_1 or S_1 are involved, the sample resistance is much higher than the tunnel barrier resistance and can be directly measured from the $I(V)$ curve. A value of $R_S=1.0\pm0.3$ GΩ is derived for both positive and negative surface voltages in the +5 to −1 V range. On the contrary, below −1 V, i.e., in the energy range of the S_2 surface state, the usual tunnel behavior is observed in the $I(V)$ curves, even at small tip-surface distances. This indicates that in this energy range, R_S has a negligible value compared to the tunnel resistance.

In this discussion, we will show that conductivity on SiC is mainly confined to the surface. We recall that the surface states U_1, S_1, and S_2 have energies located within the bulk band gap (3.0 eV width[21]), which extends from −2 to +1 eV relative to the Fermi level. It follows that the tunnel current through the three surface states cannot easily flow through the bulk. Promotion of electrons from the valence band to the S_2 or S_1 states or holes from the conduction band to the U_1 state would require a too high energy (>0.5 eV). Evidence for the electrons flowing across the surface is provided by the fact that the measured resistance, $R_S=1.0\pm0.3$ GΩ relative to the U_1 and S_1 surface states, is obtained for very high quality surfaces. The effective resistance is thus not a local measurement since it depends on the global quality of the reconstruction and not on the particular position of the measurement. Indeed, the resistance does not depend on the tip since tungsten and silver tips give the same values. This supports the idea that the electrons travel along the surface over long distances and thus act as a probe of the global quality of the reconstruction. The electronic leakage from the surface to the bulk may occur via electron-defect or electron-phonon scattering.[27–29]

Linear $I(V)$ spectra, as seen in Fig. 2(b), for small tip-surface distances have been observed as well by Gasparov *et al.*[20] close to the Fermi level but they proposed a different interpretation. They speculated that the tip proximity effect could strongly modify the electronic local density of states, leading to a destruction of the Hubbard gap with the formation of a metal/vacuum/metal (MVM) junction instead of a metal/vacuum/semiconductor (MVSc) junction. Note that a linear behavior is indeed expected for a MVM junction but only at low voltage and it does not explain the clear asymmetry between positive and negative sample biases in Fig. 2(b). Here, we are clearly in the situation of a MVSc junction where the semiconductor has a wide band gap.

The $I(Z)$ results (Sec. III B) and the $I(V)$ results at small tip-surface distances indicate that the charge transport is strongly limited by a high resistance across the correlated U_1 and S_1 surface states, whereas there seems to be no charge transport limitation across the noncorrelated S_2 surface state. However, at this point, there is no definitive proof that at −1.5 V, the current is actually flowing specifically across the S_2 surface state. Ramachandran and Feenstra[17] suggested that "dopant induced" components of the tunneling current could occur at a negative sample bias in *n*-type doped semiconductors when the tip-sample distance decreases and might play a role. It is not clear that such a dopant induced tunneling current could contribute to the high tunnel current, which can be measured at a surface voltage of −1.5 V.

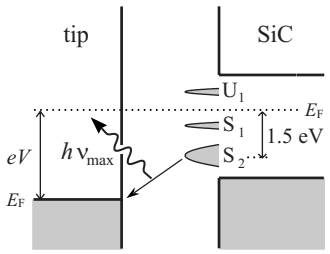

FIG. 3. Schematic of the tunnel barrier between the STM tip and the 6*H*-SiC sample showing at negative surface voltage the inelastic tunneling of electrons from the occupied S_2 surface states to the unoccupied states of the tip. The inelastic tunneling results in light emission.

D. Luminescence measurements

To clearly demonstrate that large currents can be transported through the S_2 surface state, we have detected the luminescence emitted by the STM tip-sample junction. It is known that inelastic electronic transitions between surface states of the sample and the STM tip can generate light emission whose maximum photon energy is $h\nu_{\max}=|eV|-|E_S|$, where V is the surface voltage and E_S is the energy of the surface state[30–32] relative to the Fermi energy (Fig. 3). In other words, analyzing the light emission allows the energy of the surface states involved in the tunnel current transport to be deduced. Figure 4 shows a series of luminescence spectra recorded at various sample voltages from −3.5 to −4.75 V. The cutoffs can be straightforwardly measured by enlarging the y axis. The values were taken at the point where the signal rose above the noise. This procedure had been validated on a Ag(111) surface. Thus, a number of series of precise values of $h\nu_{\max}$ could be obtained at different currents on different samples with different Ag tips. The zoom (inset Fig. 4) shows the distribution of points from many series; the distribution does not depend on the tunnel current, rather, it appears to depend on the tip. Indeed, sharp plasmon resonances are sometimes observed depending on the tip apex geometry, which make the estimation of precise and reliable cutoff values difficult. The values reported here are those corresponding to quite uniform spectra over the visible spectral range, as presented in Fig. 4, where sharp plasmon resonances are absent.

There are two interesting features. First, the maximum photon energy $h\nu_{\max}$ linearly varies as a function of the sample voltage. As the inset of Fig. 4 shows, $h\nu_{\max}$ is always smaller than $|eV|$ by around 1.5 eV. This indicates that what-

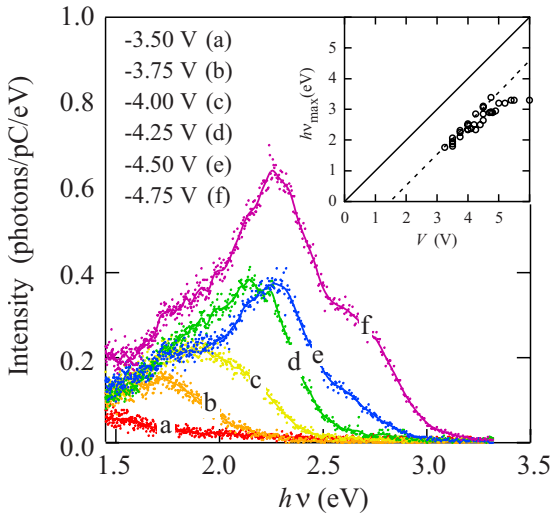

FIG. 4. (Color online) Dispersed luminescence spectra recorded at different sample voltages (−3.5, −3.75, −4.00, −4.25, −4.50, and −4.75 V). The inset shows the maximum photon energy ($h\nu_{max}$) as a function of the sample voltage (V) for many series taken at different currents, on different surfaces with different Ag tips. The spread of points gives an indication of the dispersion.

ever the tunnel current is (in the range of 3–25 nA), the luminescence is produced by inelastic tunneling from the S_2 surface state located 1.5 eV below the Fermi level of the sample (Fig. 3). Second, 1.5 eV appears to be the upper limit (dotted line in the inset). Larger offset values are possible (due to the tip) but not less. The deviation from the straight line at higher voltage (>5 eV) is due to the cutoff of the light-detection setup at a higher energy. Due to a limitation in the photon collection efficiency, the luminescence spectra could be detected after dispersion by the spectrometer only for tunnel currents higher than approximately 3 nA. A more sensitive luminescence intensity measurement was obtained by replacing the grating of the spectrometer by a mirror. In this way, the luminescence intensity could be monitored over a broader range of tunnel currents, in particular, for tunnel currents smaller than 3 nA, at both positive and negative sample voltages, as shown in Fig. 5. It is most interesting to compare the two curves in Figs. 5(a) and 5(b) recorded at sample voltages of +4.5 and −4.5 V, respectively. At a positive voltage of +4.5 V, U_1 is the only surface state available

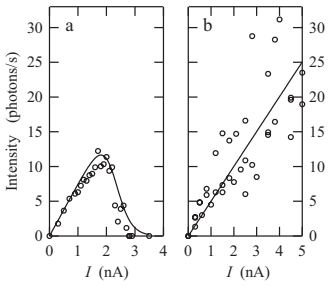

FIG. 5. Luminescence photon intensity as a function of the tunnel current for two values of the sample voltage: (a) $V=+4.5$ V and (b) $V=-4.5$ V. The solid lines are the best fits to the experimental data.

for electron transport. For tunnel currents in the 0–1 nA range, the luminescence intensities are very similar at both +4.5 and −4.5 V voltages. This indicates that the inelastic tunneling processes producing luminescence have similar cross sections at both positive and negative surface voltages. However, the luminescence associated with the inelastic tunneling into the U_1 surface state and recorded at a sample voltage of +4.5 V [Fig. 5(a)] surprisingly vanishes as soon as the tunnel current reaches 3 nA. This can be explained by the high resistance (1.0 GΩ) across the U_1 surface state resulting in a voltage drop of 3 V across the surface and a surface voltage under the STM tip of only 1.5 V. This effective surface voltage is insufficient to induce light emission in our detection wavelength range. This drop of voltage across the surface and subsequent decrease of the detected luminescence indicates that, even at +4.5 V, the tunnel current mainly flows through the U_1 state. Other tunneling channels should be negligible. Luminescence spectra were taken at two other voltages, namely, +4 and +5 V. While the cutoff is clear from the spectra, the value is variable (±0.5 nA) for a particular voltage, essentially due to tip changes. This variability means that the cutoffs measured at +4 and +5 V do not give clear enough information to confirm if the current changed in accordance to the applied voltage. Furthermore, at the lower voltage (+4 V), the wavelength range of the grating is a limiting factor.

We note that for positive surface voltages, the saturation of the tunnel current in the $I(Z)$ curves, the linear behavior of the $I(V)$ curve at a short tip-sample distance, and the luminescence measurements lead to the same conclusion of a high resistance (1.0 GΩ) across the surface. At the high voltages of +4.5 or −4.5 V, the tip is further from the surface so that even with higher currents, we would expect that tip-induced band bending is reduced compared to a set point of +2 V and 1 nA. At a negative surface voltage of −4.5 V, the luminescence intensity associated with the S_2 state shows a linear increase as a function of the tunnel current up to 5 nA [Fig. 5(b)]. This is markedly different from the behavior of the luminescence intensity associated with the U_1 state [Fig. 5(a)]. Here, we find that the luminescence intensity is proportional to the tunnel current flowing across the S_2 surface state. The result in Fig. 5(b) indicates that the drop of potential across the surface is negligible for high current flowing through the S_2 state in contrast to the U_1 and S_1 states. This precludes the opening of new tunneling channels that could be induced by dopant atoms. By deduction, for $V \leqslant -1.5$ V, the majority of the tunnel current flows through the S_2 state and the resistance through the S_2 surface state is negligible (<0.03 GΩ). Indeed, tunnel currents up to 50 nA (upper limit of our tunnel current detection) could be measured at $V=-1.5$ V.

These markedly different resistances associated with the U_1 (1.0 GΩ), S_1 (1.0 GΩ), and S_2 (<0.03 GΩ) surface states have interesting consequences. Indeed, we have seen that for $V>0.5$ V, the current mainly flows through the U_1 surface state, provided that the tunnel current is lower than V/R_S ($R_S=1.0$ GΩ). Over the range $-1.5\ \text{V} < V < -0.5$ V, the current flows only through S_1 (provided that the current is lower than V/R_S). For $V<-1.5$ V, the current mainly flows through the S_2 surface state. This is schematically summa-

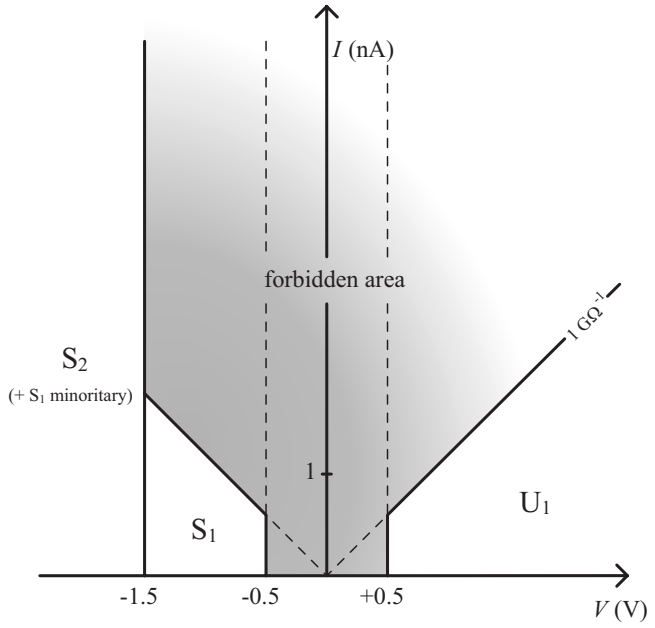

FIG. 6. Schematic diagram representing the (I,V) space of set points for STM experiments on a $6H$-SiC(0001)-3×3 surface. The dark area corresponds to set points for which tunneling is not possible, thus inducing tip-surface contact. In each white area, tunneling is limited to a specific surface state (U_1, S_1, and S_2).

rized in Fig. 6. Note that the forbidden area (dark gray shading) indicates the range of tunneling conditions where the set-point current is unattainable and the feedback loop will drive the tip into the surface. It follows that the surface state channel for electron transport can be selected at will by properly choosing the sample voltage and tunnel current.

IV. CONCLUSION

In conclusion, by combining current and luminescence measurements with the STM, we have demonstrated that the U_1, S_1, and S_2 surface states of $6H$-SiC(0001)-3×3, with energies inside the bulk band gap, have very different electronic transport properties. The unoccupied U_1 and occupied S_1 surface states derived from strongly localized and correlated electronic states at the Si adatom sites display high resistances (1.0 GΩ). On the contrary, the noncorrelated occupied S_2 surface state has a negligible resistance ($<$0.03 GΩ). This shows that the localization and electron correlation in surface states plays a clear role in surface conduction. The high resistance of the U_1 and S_1 states depends on the global quality of the surface, i.e., on the density of surface defects. Consequently, current can be selectively transported through any of these surface states. The development of these new concepts may lead to applications in multichannel nanoelectronic devices. For example, the sensitivity of each surface state conductance to the adsorption of various types of molecules can be very different,[33] thus offering the possibility to design a multichannel nanoelectronic device for gas sensing.

ACKNOWLEDGMENTS

This work is supported by the European Integrated project PICO-INSIDE (Contract No. FPG-015847), the ANR project N3M (Contract No. ANR-05-NANO-020-01), and the C'Nano program of the Région Ile de France.

[1] S. Heike, S. Watanabe, Y. Wada, and T. Hashizume, Phys. Rev. Lett. **81**, 890 (1998).
[2] T. Tanikawa, I. Matsuda, T. Kanagawa, and S. Hasegawa, Phys. Rev. Lett. **93**, 016801 (2004).
[3] P. Maksymovych, D. B. Dougherty, X.-Y. Zhu, and J. T. Yates, Phys. Rev. Lett. **99**, 016101 (2007).
[4] E. Dupont-Ferrier, P. Mallet, L. Magaud, and J.-Y. Veuillen, Phys. Rev. B **75**, 205315 (2007).
[5] P. Zhang, E. Tevaarwerk, B.-N. Park, D. E. Savage, G. K. Celler, I. Knezevic, P. G. Evans, M. A. Eriksson, and M. G. Lagally, Nature (London) **439**, 703 (2006).
[6] A. K. Geim and K. S. Novoselov, Nat. Mater. **6**, 183 (2007).
[7] S. Y. Zhou, G.-H. Gweon, A. V. Fedorov, P. N. First, W. A. de Heer, D.-H. Lee, F. Guinea, A. H. Castro Neto, and A. Lanzara, Nat. Mater. **6**, 770 (2007).
[8] M. V. Fistul and K. B. Efetov, Phys. Rev. Lett. **98**, 256803 (2007).
[9] M. Lastapis, D. Riedel, A. Mayne, K. Bobrov, and G. Dujardin, Low Temp. Phys. **29**, 196 (2003).
[10] R. M. Feenstra, S. Gaan, G. Meyer, and K. H. Rieder, Phys. Rev. B **71**, 125316 (2005).
[11] G. Dujardin, A. J. Mayne, and F. Rose, Phys. Rev. Lett. **89**, 036802 (2002).
[12] J. Ristein, F. Maier, M. Riedel, M. Stammer, and L. Ley, Diamond Relat. Mater. **10**, 416 (2001).
[13] K. Bobrov, A. J. Mayne, G. Comtet, G. Dujardin, L. Hellner, and A. Hoffman, Phys. Rev. B **68**, 195416 (2003).
[14] L. Hellner, A. J. Mayne, R. Bernard, and G. Dujardin, Diamond Relat. Mater. **14**, 1529 (2005).
[15] J. A. Garrido, T. Heimbeck, and M. Stutzmann, Phys. Rev. B **71**, 245310 (2005).
[16] G. Profeta and E. Tosatti, Phys. Rev. Lett. **98**, 086401 (2007).
[17] V. Ramachandran and R. M. Feenstra, Phys. Rev. Lett. **82**, 1000 (1999).
[18] J. Furthmüller, F. Bechstedt, H. Hüsken, B. Schröter, and W. Richter, Phys. Rev. B **58**, 13712 (1998).
[19] J. E. Northrup and J. Neugebauer, Phys. Rev. B **57**, R4230 (1998).
[20] V. A. Gasparov, M. Riehl-Chudoba, B. Schröter, and W. Richter, Europhys. Lett. **51**, 527 (2000).
[21] L. S. O. Johansson, L. Duda, M. Laurenzis, M. Krieftewirth, and B. Reihl, Surf. Sci. **445**, 109 (2000).
[22] F. Amy, H. Enriquez, P. Soukiassian, C. Brylinski, A. Mayne, and G. Dujardin, Appl. Phys. Lett. **79**, 767 (2001).
[23] J. Schardt, J. Bernhardt, U. Starke, and K. Heinz, Phys. Rev. B **62**, 10335 (2000).
[24] F. Amy, H. Enriquez, P. Soukiassian, P.-F. Storino, Y. J. Chabal, A. J. Mayne, G. Dujardin, Y. K. Hwu, and C. Brylinski, Phys.

Rev. Lett. **86**, 4342 (2001).
[25] J. Stroscio and W. J. Kaiser, *Scanning Tunneling Microscopy* (Academic, New York, 1993).
[26] F. Flores and N. García, Phys. Rev. B **30**, 2289 (1984).
[27] T. Tanikawa, K. Yoo, I. Matsuda, S. Hasegawa, and Y. Hasegawa, Phys. Rev. B **68**, 113303 (2003).
[28] K. Yoo and H. H. Weitering, Phys. Rev. B **65**, 115424 (2002).
[29] J. W. Wells, J. F. Kallehauge, T. M. Hansen, and Ph. Hofmann, Phys. Rev. Lett. **97**, 206803 (2006).
[30] R. Berndt, J. K. Gimzewski, and P. Johansson, Phys. Rev. Lett. **67**, 3796 (1991).
[31] S. Kagami, H. Minoda, and N. Yamamoto, Surf. Sci. **493**, 78 (2001).
[32] M. Sakurai, C. Thirstrup, and M. Aono, Appl. Phys. A: Mater. Sci. Process. **80**, 1153 (2005).
[33] G. Baffou, A. J. Mayne, G. Comtet, and G. Dujardin, Appl. Phys. Lett. **91**, 073101 (2007).